Cation Distribution in Lithium Nickel Oxide Crystals

M. A. Monge,*[,1a] E. Gutiérrez-Puebla,[1a] J. L. Martínez,[1a] I. Rasines,[1a] and J. A. Campa[1b]

Instituto de Ciencia de Materiales de Madrid, Consejo Superior de Investigaciones Científicas, Cantoblanco, E-28049 Madrid, Spain, and Facultad de Ciencias Geológicas, Universidad Complutense, E-28040 Madrid, Spain

Received February 22, 2000. Revised Manuscript Received April 7, 2000

Octahedral black-colored $Li_{0.27}Ni_{0.73}O$ crystals were ground and studied by single-crystal X-ray diffraction. They crystallize in the rhombohedral *R*3 space group (no. 146) with unit cell dimensions (Å) $a = 6.020(2)$ and $c = 14.726(5)$. The crystal structure consists of a close-packing oxygen arrangement with the cations occupying all of the octahedral sites, in such a way that two mixed layers containing Li and Ni in different proportions alternate along the *c* direction. The Li ordering is incompatible with the existence of pure Ni layers alternating with more or less doped Li ones as was assumed in the model admitted until now. The new model looks consistent with the magnetization measurements (300−2 K), which give evidence that $Li_{0.27}Ni_{0.73}O$ behaves as a mictomagnetic material, and can throw some light upon the Li diffusion pathway in rechargeable batteries.

Introduction

Although polycrystalline $LiNiO_2$ was prepared and studied[2] for the first time in the 1950s, it currently raises considerable attention in the fields of electrochemistry, catalysis, and magnetism. It is also interesting from a practical point of view, because it could replace more expensive $LiCoO_2$ as cathode material for long-life 4 V rechargeable lithium batteries and for intermediate temperature fuel cells. In fact a recent electrochemical test of a half-cell performed using $LiNiO_2$ powders has shown[3] that the cell had a high initial discharge capacity, 158 mA h g^{-1}, but it showed very fast capacity fading just after several tens of charge/discharge cycles. It has also been shown[4] that when used as cathode material, $LiNiO_2$ exhibits higher electrical conductivity and better H_2/O_2 fuel cell performance than $LiCoO_2$, although its thermal stability at intermediate temperatures is relatively poorer than that of the latter.

Pure $LiNiO_2$ completely exempt of Ni(II) has never been obtained. Its actual composition, $Li_xNi(II)_{1-2x}Ni(III)_xO$, used to be formulated as it was initially[5] written, $Li_xNi_{1-x}O$. For small *x* values, $0 < x \leq 0.2$, this material keeps the rock-salt structure type of NiO. For larger *x*, $0.2 < x < 0.5$, it adopts rhombohedral symmetry and was refined[5] in the space group (S. G.) $R\bar{3}m$ (no. 166) with Li at 3*a* (0,0,0), Ni at 3*b* (0,0,1/2), O at 6*c* (0,0,*z*), and $z \cong 0.25$. Rhombohedral $Li_xNi_{1-x}O$ can be conceived as a close packing of oxide anions which alternate with ordered layers of Ni and Li parallel to the (111) plane of the parent cubic NiO lattice. Many Rietveld profile refinements of X-ray and neutron diffraction data have confirmed this model, although some[6−8] of them have detected the presence of a fraction of Ni atoms in the Li layers.

The magnetic properties of $Li_xNi_{1-x}O$ have been interpreted in all the ways imaginable, most probably because a variety of chemical compositions of this material occur depending on the synthesis conditions, and because the magnetization measurements were performed on polycrystalline samples of different qualities.[9−11] Taking into account that there also exist references[12−15] to various monoclinic and hexagonal phases related to rhombohedral $Li_xNi_{1-x}O$ and that the samples used for all the published investigations on $Li_xNi_{1-x}O$ were powders, we proposed to grow crystals of this material, with a view to obtain more information on its crystal structure and intrinsic physical properties.

(1) (a) Consejo Superior de Investigaciones Científicas. (b) Universidad Complutense.

(2) Dyer, L. D.; Borie, B. S.; Smith, G. P. *J. Am. Chem. Soc.* **1954**, *76*, 1499.
(3) Lee, Y. S.; Sun, Y. K.; Nahm, K. S. *Solid State Ionics* **1999**, *118*, 159.
(4) Tao, S.; Wu, Q.; Zhan, Zh; Meng. G. *Solid State Ionics* **1999**, *124*, 53.
(5) Goodenough, J. B.; Wickham, D. G.; Croft, W. J. *J. Phys. Chem. Solids* **1958**, *5*, 107.
(6) Bajpai, A.; Banerjee, A. *Phys. Rev. B* **1997**, *55*, 12439.
(7) Hirano, A.; Kanno, R.; Kawamoto, Y.; Takeda, Y.; Yamaura, K.; Takano, M.; Ohyama, K.; Ohashi, M.; Yamaguchi, Y. *Solid State Ionics* **1995**, *78*, 123.
(8) Massarotti, V.; Capsoni, D.; Bini, M.; Mustarelli, P.; Marini, S. *Ionics* **1995**, *1*, 421.
(9) Shirakami, T.; Takematsu, M.; Hirano, A.; Kanno, R.; Yamaura, K.; Takano, M.; Atake, T. *Mater. Sci. Eng., B* **1998**, *4*, 70.
(10) Yamaura, K.; Takano, M.; Hirano, A.; Kanno, R. *J. Solid State Chem.* **1996**, *127*, 109.
(11) Takematsu, M.; Shirakami, T.; Atake, T.; Hirano, A.; Kanno, R. In *Solid State Ionics: New Developments*; Chowdari, B. V. R., Ed.; World Scientific: Singapore, 1996; p 330.
(12) Li, W.; Reimers, J. N.; Dahn, J. R. *Solid State Ionics* **1993**, *67*, 123.
(13) Hirano, A.; Kanno, R.; Kawamoto, Y.; Oikawa, K.; Kamiyama, T.; Izumi, F. *Solid State Ionics* **1996**, *86−88*, 791.
(14) Delmas, C.; Peres, J. P.; Rougier, A.; Demourgues, A.; Weill, F.; Chadwick, A.; Broussely, M.; Perton, F.; Biensan Ph.; Willmann, P. *J. Power Sources* **1997**, *68*, 120.
(15) Peres, J. P.; Weill, F.; Delmas, C. *Solid State Ionics* **1999**, *116*, 19.

10.1021/cm0010203 CCC: $19.00
Published on Web 06/23/2000

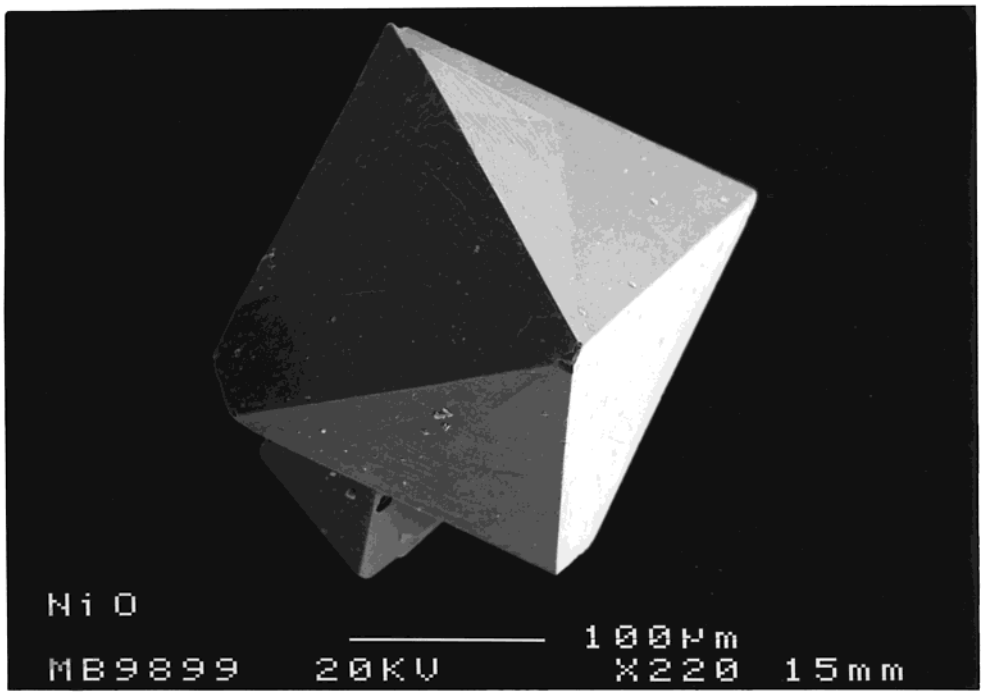

Figure 1. One $Li_{0.27}Ni_{0.73}O$ crystal showing 0.2 mm edges.

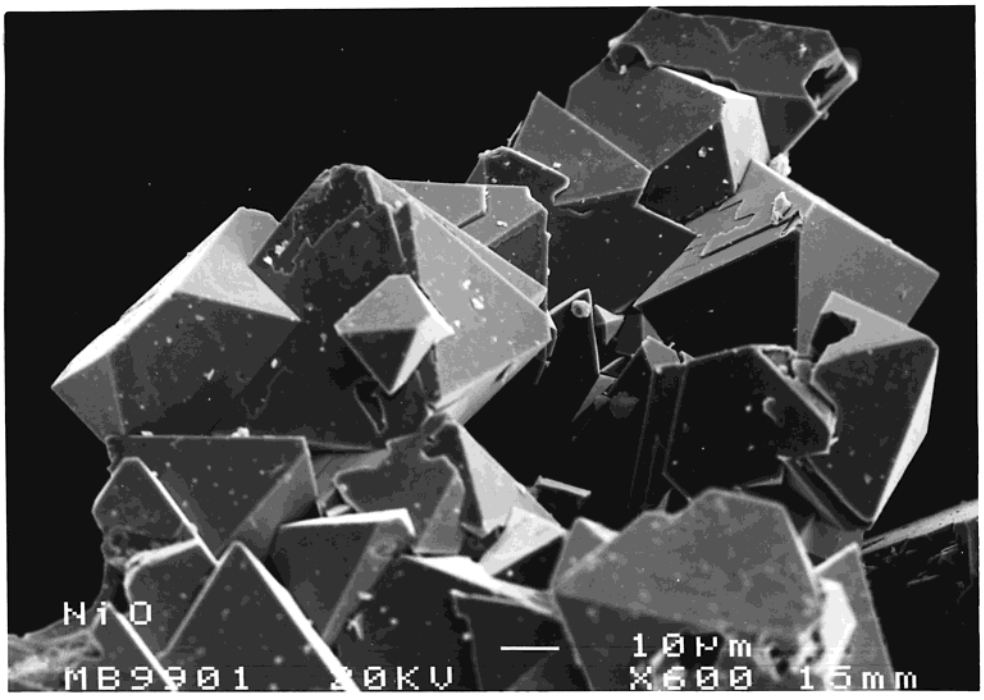

Figure 2. Small $Li_{0.27}Ni_{0.73}O$ crystals as grown.

This paper includes the results of our attempts, viz., the growth of $Li_{0.27}Ni_{0.73}O$ single crystals, the solution of their crystal structure, and evidence on the behavior of $Li_{0.27}Ni_{0.73}O$ as a mictomagnetic material. The crystal structure, which is the first example of a novel structure type model, includes the alternation of mixed layers both containing Li and Ni in different proportions. The model shows how the way in which the Li atom tends to ordinate itself forces the appearance of a new cell and excludes the existence of pure Ni layers alternating with more or less doped Li ones. On the other hand, the present model for $Li_{0.27}Ni_{0.73}O$ looks consistent with its magnetic properties, and can throw some light upon the Li diffusion pathway in Li batteries.

Experimental Section

Crystal Growth. The attempts at growing single crystals were performed using platinum crucibles and reagent grade products. Mixtures of NiO and $Li_2SO_4 \cdot H_2O$ or Li_2CO_3 heated at 1200 °C yielded NiO crystals. Mixtures of NiO with $LiBO_2$, Li_2CO_3, and K_2SO_4 or with $LiBO_2$, $Li_2SO_4 \cdot H_2O$, Li_2CO_3, and Na_2SO_4 were unsuccessful too. Finally mixtures of NiO, $LiBO_2$, and some R_2O_3 (R = Y, La, Nd, Gd) led to octahedral black-colored crystals of $Li_{0.27}Ni_{0.73}O$ (Figures 1 and 2). The samples used for crystal structure determinations and magnetization

Table 1. Crystal Data and Structure Refinement for $Li_{0.27}Ni_{0.73}O$

fw (g formula^{-1})	60.72	cryst size (mm)	0.4 × 0.3 × 0.2
temp (K)	153(2)	θ range for data collection (deg)	4.15−23.08
wavelength (Å)	0.710 73	limiting indices	$-2 \le h \le 6$, $-6 \le k \le 6$, $-4 \le l \le 16$
cryst syst	rhombohedral	no. of reflns collected	375
space group	*R*3 (no. 146)	no. of independent reflns	186 (R_{int} = 0.1069)
unit cell dimensions	a = 6.020(2) Å, α = 90°	refinement method	full-matrix least-squares on F^2
	b = 6.020(2) Å, β = 90°	no. of data/restraints/params	186/0/40
	c = 14.726(5) Å, γ = 120°	goodness of fit on F^2	0.982
vol (Å^3)	462.1(2)	final R indices [$I > 2\sigma(I)$]	R1 = 0.0723, wR2 = 0.2396
Z (formula (unit cell)$^{-1}$)	24	R indices (all data)	R1 = 0.0829, wR2 = 0.2540
density (calcd) (Mg m^{-3})	5.327	absolute structure param	0.1(6)
abs coeff (mm^{-1})	19.973	extinction coefficient	0.07(4)
F(000)	510	largest difference peak and hole (e Å^{-3})	1.954 and −1.395

experiments showed edges of 0.2−0.3 mm and were grown from one mixture of 10 g of $LiBO_2$, 1 g of Nd_2O_3, and 0.5 g of NiO. This mixture was heated until 1200 °C at 4 °C h^{-1}, soaked for 2 h, and cooled at 4 °C h^{-1} to 920 °C and subsequently to room temperature, turning the power off.

X-ray Structure Determinations. With regard to the desired quality of the results, special care was paid to the selection of single crystals. Each of those chosen was tested for perfection and scattering power on a Brucker-Siemens SMART diffractometer equipped with a CDC bidimensional detector, and normal focus 2.4 kW sealed tube as X-ray source (graphite-monochromated molybdenum radiation, λ = 0.710 73 Å) operating at 50 kV and 20 mA. Two black crystals showing well-defined faces were finally chosen and fully analyzed, giving practically identical refinements (positions, site occupancies, etc.). The two selected cystals were mounted on the named diffractometer, and their data were collected over a quadrant of the reciprocal space by a combination of two exposure sets. Each exposure of 10 s covered 0.3° in ω. The crystal to detector distance was 6.05 cm. Coverage of the unique set was over 92% complete to at least 23° in θ, in both cases. The first 50 frames were recollected at the end of the data collection to monitor crystal decay. The unit-cell dimensions were determined by using the whole set of reflections and refined by least-squares refinement for both crystals. The intensities were corrected for Lorentz and polarization effects. Scattering factors for neutral atoms and dispersion corrections for Ni were taken from the *International Tables for Crystallography*.[16] The structure was solved by Multan and Fourier methods. Full-matrix least-squares anisotropic refinement was carried out minimizing $w(F_o^2 - F_c^2)$. Most of the calculations were carried out with SMART[17] software for data collection and data reduction, and SHELXTL[17] for structure solution and refinements. A summary of the fundamental crystal and structure data is given in Table 1. All these data refer to the crystal that gave a slightly lower R value at the end of the refinement.

Powder Diffraction Pattern. The X-ray powder diffraction pattern was obtained by using a Siemens Kristalloflex 810 generator, a D-500 goniometer provided with a graphite monochromator, and Cu Kα radiation (λ = 1.5406 Å). The d spacing measurements were performed at 0.2° (2θ) min^{-1} for 10° < 2θ < 135°, using wolfram, a = 3.165 24(4), as an internal standard. Unit cell parameters were refined from the 2θ values of the last 12 observed reflections. The intensities were measured by step-scanning from 10° to 120° (2θ) with increments of 0.05° (2θ) and a counting time of 4 s each step, the goniometer being controlled by a DACO-MPV2 computer, which carried out the integration of the diffraction peaks and the background correction.

Magnetic Measurements. A SQUID magnetometer (Quantum Design) operating from 300 to 2.0 K at various fields between 1 and 50 kOe was used to perform the dc magnetic measurements in single crystals of $Li_{0.27}Ni_{0.73}O$ under field cooling, FC, and zero-field cooling, ZFC, conditions. Diamagnetic corrections for magnetic susceptibilities[18] were taken into account. The field dependence of magnetization was measured in magnetic fields ranging from −40 to +40 kOe at temperatures of 5, 40, 110, and 200 K, and the ac magnetic susceptibility was determined with an alternating field of 1 Oe in amplitude at various frequencies between 0.01 and 1 kHz.

Table 2. Atomic Coordinates (×10^4), Positions, Equivalent Isotropic Displacement Parameters (Å^2 × 10^3), and Population Factors (pf) for $Li_{0.27}Ni_{0.73}O$

atom	position	x	y	z	U_{eq}[a]	pf
Ni(1)	3a	6667	3333	2279(92)	13(5)	1.00
Ni(2)	9b	4982(25)	4984(23)	3993(76)	12(5)	1.00
Ni(3)	9b	8273(69)	6671(65)	5531(66)	42(9)	0.52(5)
Ni(4)	3a	0	0	3997	16(18)	0.24(8)
Li(1)	9b	8273(69)	6671(65)	5531(66)	42(9)	0.48(5)
Li(2)	3a	0	0	3997	16(18)	0.76(8)
O(1)	3a	6667	3333	4758(84)	1(22)	1.00
O(2)	9b	1628(62)	3319 (50)	4737(90)	42(40)	1.00
O(3)	3a	3333	6667	3147	79(58)	1.00
O(4)	9b	3530(57)	1791(53)	3171(67)	18(13)	1.00

[a] U_{eq} is defined as one-third of the trace of the orthogonalized U_{ij} tensor.

Results and Discussion

Crystal Structure of $Li_{0.27}Ni_{0.73}O$. From a study of the weak reflections in the spectrum, the new hexagonal cell of parameters a = 6.020(2) Å and c = 14.726(5) Å became evident. Weak reflections unambiguously indexed in this unit cell, 1 2 −4 or −1 3 −4 for instance, could not have been indexed in the smaller one[2,5] with unit cell parameters a = 2.88 Å and c = 14.2 Å. The space group *R*3 (no. 146) was obtained during the course of the structure solution after hexagonal groups in which the only extinction is $-h + k + l \neq 3n$ were tried. In this space group anisotropic refinement for most of the atoms was performed. The small difference between the R value of 0.07 for observed reflections, $I > 2\sigma(I)$, and the R value of 0.08 for all reflections indicates the goodness of the model for the weak reflections too.

Three positions have been found for the Ni atoms in the asymmetric unit (Table 2). Two of these positions, Ni(1) and Ni(2), are fully occupied by Ni. The refined population factor for Ni(3) was 0.55(5), equivalent to an electron density of 15.4(14) e$^-$. This density can be generated by sharing either half of a nickel atom, Ni(3), and half of a lithium atom, Li(1), or by 55% nickel, Ni(3), and 45% vacants. There is one site occupied mainly by lithium, the population factors at this site being 0.76(8) for Li, Li(2), and 0.24(8) for Ni, Ni(4). In

(16) *International Tables for Crystallography*; Wilson, A. J. C., Ed.; Kluwer: Dordrecht, The Netherlands, 1995; Vol. C, pp 219 and 477.

(17) SMART and SHELXTL, Siemens Energy and Automation Inc., Analytical Instrumentation, Karlsruhe, Germany, 1996.

(18) Boudreaux, E. A.; Mulay L. N. *Theory and Applications of Molecular Paramagnetism*; Wiley: New York, 1976; pp 494−495.

Table 3. X-ray Powder Diffraction Pattern for Rhombohedral $Li_{0.27}Ni_{0.73}O$ with Hexagonal Unit cell Parameters (Å) $a = 6.0136(6)$ and $c = 14.747(5)$

hkl	*d* Å	I_{obsd}
003, 101	4.910	100
015, 113	2.570	29
006, 202	2.457	97
024	2.1267	88
107, 205, 211	1.9521	19
027, 125, 303	1.6350	26
208	1.5045	17
220	1.5032	2
119, 217, 131	1.4383	12
0 2 10	1.2828	9
226, 042	1.2820	9
0 0 12	1.2287	5
404	1.2270	13
2 0 11, 309, 137, 321	1.1910	3
048	1.0639	4
2 2 12	0.95152	4
244	0.95092	4

no case did the electron density found correspond to even traces of the Nd_2O_3 from the flux.

The standard deviations (Table 2) denounce some nonresolvable disorder involving O(3) due to the fact of being in the polyhedron of a shared position. The high standard deviation of Li(2) can be attributed to the small electron density at its site. Nevertheless, the existence of some modulation along the *c* direction as it happens in other nickel oxides along the packing direction[19] is not discarded.

Taking into account the two possibilities arising from the refinement for the Ni(3) site, two formulas derive from the refinement: (I) without vacants, $Li_{0.27}Ni_{0.73}O$, where the Ni average charge is 2.37, and (II) with vacants, $Li_{0.10}Ni_{0.74}O$, and a Ni charge of 2.57. Concerning (I), it has to be said that in no moment were the total amounts of Ni and Li in the formula constrained to the unit. Nevertheless, in the obtained composition, $Li_{0.27}Ni_{0.73}O$, there are no vacants, despite having refined the population factor in two separate shared positions. The results of the final refinement have been deposited.[20]

The *d* spacings from the X-ray powder diffraction data for $Li_{0.27}Ni_{0.73}O$ (Table 3) coincide with those calculated[21] assuming the same stoichiometry, space group, atomic positions, and site occupations obtained after the single-crystal structure was solved. With the exception of reflections such as 003 and 006 in which preferential orientation can be present, the agreement between observed and calculated intensities is also good. The unit cell parameters observed for polycrystalline $Li_{0.27}Ni_{0.73}O$ are $a = 6.0136(6)$ Å and $c = 14.747(5)$ Å. These parameters are interdependent since $c^2 \cong a^3$ up to a high degree of accuracy. Taking this into account and that $a \cong 6$ Å, the expression $d = c\{[4/3(c/a)^2(h^2 + hk + k^2)] + l^2\}^{-1/2}$, which gives the *d* values as a function of the *a* and *c* unit cell dimensions and the hexagonal *hkl* Miller indexes, becomes $d = c[8(h^2 + hk + k^2)] + l^2]^{-1/2}$. As a result, the reflections for which the *s* values, $s = 8(h^2 + hk + k^2) + l^2$, are equal have the same *d* spacing: for instance (Table 3) 003 and 101, 015 and 113, and so on. A good number of these sets of reflections could not be resolved, not even at lower scanning rates and larger counting times.

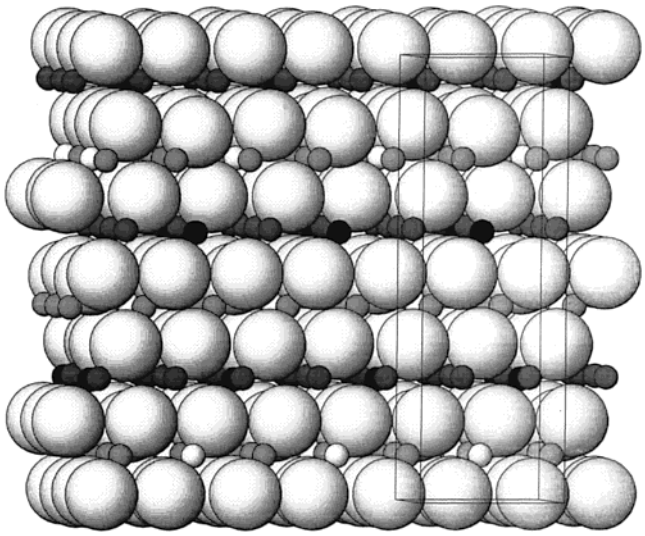

Figure 3. View of the oxygen cubic close packing of $Li_{0.27}Ni_{0.73}O$ along *c* following the ABC layer sequence. The small spheres lie at positions occupied only by nickel, Ni(1) and Ni(2), (black), half and half by Ni(3) and Li(1) (gray), or mainly by lithium, Li(1) (white).

The structure of $Li_{0.27}Ni_{0.73}O$ can be envisaged as a close packing of oxide anions in which the cations occupy all the octahedral holes (Figure 3). The anions follow the ABC layer sequence characteristic of the cubic close packing. The unit cell volume per oxygen atom of $Li_{0.27}Ni_{0.73}O$, 19.2 Å^3, is comparable to those[22] of other close-packed oxygen arrangements such as cubic saltlike NiO, 18.2 Å^3, and lithium spinels, which vary from 16.2 to 19.6 Å^3 for $LiNi_2O_4$ and $Li_{0.3}Mn_{0.7}Ti_2O_4$, respectively.

The cations in $Li_{0.27}Ni_{0.73}O$ give rise along the *c* direction to the alternation of L1 and L2 mixed layers containing Li and Ni in different proportions. For model I, L1 is formed by Ni(2) and $[Li(2)_{0.76} + Ni(4)_{0.24}]$, and L2 is also a mixed layer constituted by Ni(1) and $[Ni(3)_{0.52} + Li(1)_{0.48}]$, with Ni:Li proportions near 4:1 and 5:3, respectively. In the case of model II, L2 would be formed by $[Ni(3)_{0.55} + \square_{0.45}]$, and the concentration of Ni vacants of 45% would likely lead to an ordering of the Ni atoms which is not detected; hence, this hypothesis looks less probable.

Figure 4 shows a view of the L1 and L2 layers that constitute the new unit cell. Different circles represent positions fully occupied by nickel, Ni(1) and Ni(2); those occupied by nickel and lithium, Ni(3) and Li(1) half and half; and those occupied mainly by lithium, Li(2), and some nickel, Ni(4). The oxygen close packing of $Li_{0.27}Ni_{0.73}O$ along *c* can be seen in Figure 4, where the small spheres lie at positions occupied only by nickel, Ni(1) and Ni(2) (black), half and half by Ni(3) and Li(1) (gray), or mainly by lithium, Li(1) (white).

From the analysis of the L1 and L2 layers (Figure 4) it becomes evident that the way in which the lithium tends to ordinate itself forces the formation of the superstructure with parameters (Å) $a = 6.0136(6)$ and

(19) Evain, M.; Boucher, F.; Gourdon, O. *Chem. Mater.* **1998**, *10*, 3068.

(20) ICSD 410837, Fachinformationszentrum Karlsruhe, Eggenstein-Leopoldshafen, D-76344.

(21) Yvon, R.; Jeitschko, W.; Parthé, E. *J. Appl. Crystallogr.* **1977**, *10*, 73.

(22) International Centre for Diffraction Data. *Powder Diffraction File*; Card Nos. 47-1049, 41-890, and 41-63.

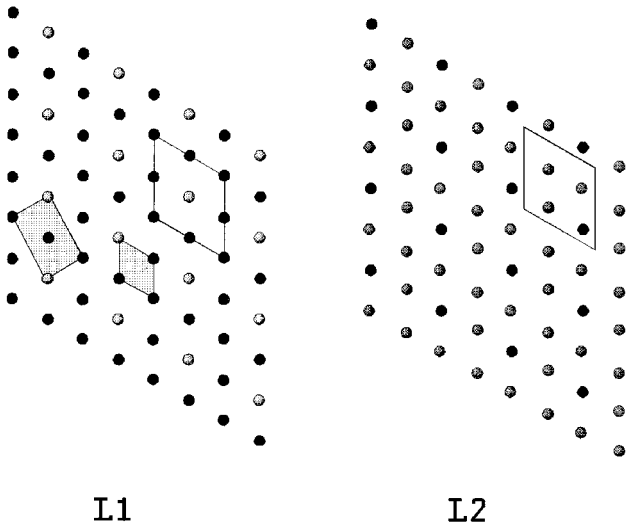

Figure 4. View of the L1 and L2 layers showing the new unit cell (white) of $Li_{0.27}Ni_{0.73}O$. Black circles represent positions fully occupied by nickel, Ni(1) and Ni(2); dark gray circles are those occupied by nickel, Ni(3), and lithium, Li(1), half and half; and light gray circles are those occupied mainly by lithium, Li(2), and some Ni(4). The shadowed small rhombohedral[2,5] and the monoclinic[15] cells are also represented.

$c = 14.747(5)$ ruling out, for the $Li_{0.27}Ni_{0.73}O$ composition, the small rhombohedral cell[2,5] of hexagonal parameters (Å) $a = 2.88$ and $c = 14.2$ as well as the monoclinic one defined in some papers.[7,12−15] In conclusion, the cation distribution in the oxygen cubic closed packing leads to the hexagonal unit cell, and the order of Li atoms in L1 and L2 gives rise to the superstructure here determined.

In a recent study[15] of electron diffraction on polycrystalline $Li_{0.32}Ni_{0.51}O$, the existence of a hexagonal unit cell with parameters twice as long as those[2,5] of small rhombohedral $Li_xNi_{1-x}O$ has been presumed, to explain a possible ordering of vacancies among the *lithium layers*. In the present paper it has been shown using single-crystal X-ray diffraction that this cell exists, although what makes the parameter double is not the ordered Li vacants but the situation of Li in the supposed Ni layer to give L1. This is shown in L1 of Figure 4 where the three unit cells have been drawn for comparison, the smaller rhombohedral[2,5] and the monoclinic,[15] both shadowed, along with that described in this paper.

Ni−O and Li−O selected distances are shown in Table 4 together with a conventional δ parameter which indicates the distortions of NiO_6 and LiO_6 octahedra. The large standard deviations which show the distances involving O(3) or Li(2) agree with the nonresolvable O(3) disorder and the high standard deviation obtained after Li(2) was refined. Taking into account the deviations obtained for distances shown in Table 4, the most irregular octahedra are $Ni(3)O_6$ and $Li(2)O_6$, with δ values of 550 and 447, respectively. These are precisely the octahedra which lie at positions shared by Ni and Li. In the $Ni(3)O_6$ octahedra two distances fairly larger than the other four can be distinguished. The shortest Ni−O distances are shown by Ni(2), of which there is a fraction of $9/17.4 = 0.52$ in the unit cell. This ratio is similar to that of Ni^{3+} to Ni^{2+}, 0.59, in $Li_{0.27}Ni_{0.73}O$. Table 4 also includes shortest Ni−Ni distances for $Li_{0.27}Ni_{0.73}O$, which are larger than in Ni metal, 2.49 Å. They vary between 2.8(2) and 3.05(5) Å, the intralayer Ni−Ni distances being slightly larger than those between layers.

The fully occupied Ni positions, Ni(1) and Ni(2), are disposed along the stacking *c* direction in such a way that each Ni(1) is surrounded by six Ni(2), three of them in the upper layer and the other three in the lower one. Similarly those sites occupied mainly by Li(2) are always located between six positions, three in each of the next layers, shared by Li, Li(1), and Ni, Ni(3). The Ni−Ni connections through oxygen triangles run not exactly along the *c* axis, but in approximately the (223) direction, because of the distribution of the octahedral sites in the cubic close packing of the anions (Figure 3). Consequently, due to the existence of ordered mixed Li/Ni layers, in this material there are not isolated Ni clusters as has been recently supposed,[23] but a disposition in which the Ni atoms are always connected through oxygens. The same connection through oxygen triangles exists among those positions occupied mainly by Li, Li(2), and those that are shared by Li and Ni (Figure 4). This fact together with the nonexistence of pure Ni layers seems to indicate that the simple idea of a 2D process for Li diffusion in this material is challenged.

Magnetic Properties of $Li_{0.27}Ni_{0.73}O$. Among numerous magnetization measurements recently performed[6,7,9−11] on polycrystalline samples of $Li_xNi_{1-x}O$, a few typical results will be mentioned here. Takematsu and co-workers[11] measured dc magnetic susceptibility on a polycrystalline sample of composition $x = 0.025$ in two fields. At 1 kOe they observed a behavior similar to that of a spin glass: below 25 K the FC susceptibility, *M*/*H*, was larger than that after ZFC, and below 10 K the FC susceptibility showed less temperature dependence, while that after ZFC had a peak at about 10 K. The behavior in a very low magnetic field, 10 Oe, was quite different: the discrepancy in magnetic susceptibility between FC and ZFC was much larger than that at 1 kOe, and was maintained up to 220 K, suggesting the existence of weak ferromagnetism, and the temperatures at which the maximum of the ZFC and FC susceptibilities appear, which were almost equal at 1 kOe, turned out to be different, about 30 and 10 K, respectively. The presence of weak ferromagnetic interactions was confirmed from curves of field dependence on magnetization at 20, 30, and 50 K. All these curves showed hysteresis loops and suggested the existence of a paramagnetic correlation such as superparamagnetism. In conclusion, the mictomagnetism of $Li_{0.475}Ni_{0.525}O$ was considered as a superposition of weak ferromagnetism and superparamagnetism.

T. Shirakami et al.[9] succeeded in preparing a sample of composition $Li_{0.495}Ni_{0.505}O$, near stoichiometric $Li_{0.5}Ni_{0.5}O$. In that sample they observed a typical spin-glass-like behavior at 10 Oe: the ZFC susceptibility showed a cusplike peak al 8 K, the FC susceptibility had little temperature dependence below 8 K, and both susceptibilities agreed above 8 K. The reciprocal dc susceptibility, *H*/*M*, measured after FC followed the Curie−Weiss law from 100 to 300 K and led to a Weiss

(23) . Merzt, D.; Ksari, Y.; Celestini, F.; Debierre, J. M.; Stepanov, A.; Delmas, C. *Phys. Rev. B* **2000**, *61*, 124.

Table 4. Selected Distances (Å) and Octahedral δ Distortions, $\delta = 10^4\Sigma(d - \bar{d})^2$, for $Li_{0.27}Ni_{0.73}O$

Ni(1)−O(2)	3 × 2.17(7)	Ni(3),Li(1)−O(1)	2.10(8)	Ni(1)−Ni(2)	3 × 2.94(4)[a]
Ni(1)−O(4)	3 × 2.12(6)	Ni(3),Li(1)−O(2)	2.05(9)	Ni(1)−Ni(3)	2 × 3.04(5)[c]
Ni(1)−O	2.14(7)	Ni(3),Li(1)−O(2′)	2.14(8)		
$\delta_{Ni(1)}$	14	Ni(3),Li(1)−O(3)	2.23(14)	Ni(2)−Ni(2)	3.02(3)[b]
		Ni(3),Li(1)−O(4)	2.27(7)	Ni(2)−Ni(3)	2.85(5)[a]
Ni(2)−O(1)	2.07(5)	Ni(3),Li(1)−O(4′)	2.32(7)	Ni(2)−Ni(3′)	2.88(5)[c]
Ni(2)−O(2)	2.03(6)	Ni(3),Li(1)−O	2.18(9)		
Ni(2)−O(2′)	2.07(6)	$\delta_{Ni(3),Li(1)}$	550	Ni(3)−Ni(3)	3.03(8)[c]
Ni(2)−O(3)	2.13(12)			Ni(3)−Ni(4)	2.8(2)[a]
Ni(2)−O(4)	2.08(6)	Li(2),Ni(4)−O(2)	3 × 2.06(14)		
Ni(2)−O(4′)	2.07(5)	Li(2),Ni(4)−O(4)	3 × 2.2(2)		
Ni(2)−O	2.07(8)	Li(2),Ni(4)−O	2.13(17)		
$\delta_{Ni(2)}$	52	$\delta_{Li(2),Ni(4)}$	447		

[a] Ni−Ni interlayer distance. [b] Ni−Ni intra-L1 distance. [c] Ni−Ni intra-L2 distance.

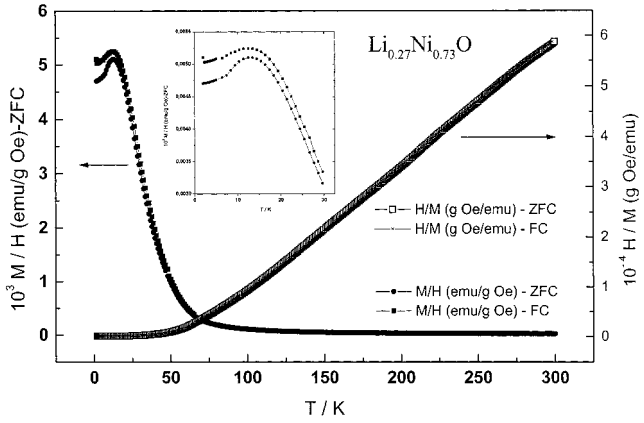

Figure 5. dc mass susceptibility, *M*/*H*, and its reciprocal, as functions of temperature, for $Li_{0.27}Ni_{0.73}O$.

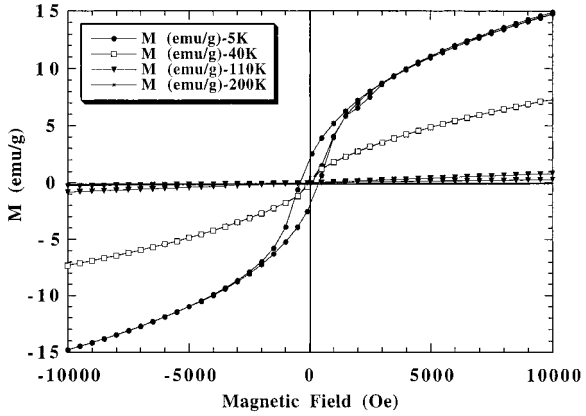

Figure 6. Field dependence of magnetization at different temperatures for $Li_{0.27}Ni_{0.73}O$.

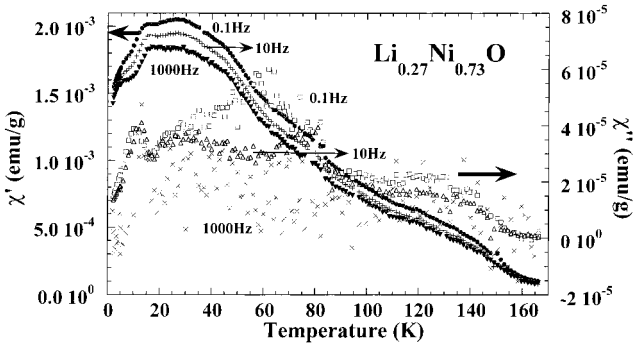

Figure 7. ac susceptibilities for $Li_{0.27}Ni_{0.73}$ measured in an alternating field of 1 Oe at frequencies (Hz) of 0.1, 10, and 1000.

constant of 31 K. According to these authors, the positive value of the Weiss constant does not necessarily imply that the exchange interaction between Ni ions is ferromagnetic.

The dc magnetic susceptibility, *M*/*H*, of $Li_{0.27}Ni_{0.73}O$ crystals and its reciprocal is represented in Figure 5. Below 28 K the susceptibility after FC is slightly larger than that after ZFC. Both ZFC and FC show a peak, broader for FC, at 14 and 12 K, respectively. Below 12 K the ZFC is more temperature dependent. For higher temperatures, in the interval 110−300 K, the reciprocal mass susceptibility, *H*/*M*, follows (R = 0.999 92) the Curie−Weiss law $X_g^{-1} = 251.00(23) - 16033(49)T$. The molar ($Li_{0.27}Ni_{0.73}O$) susceptibility gives a Curie constant of 0.3314(31) cm^3 K mol^{-1} and a Weiss temperature of 63.88(58) K. In the curve of Figure 6, which shows the field dependence of magnetization at 5 K, a hysteresis loop can be seen.

In $Li_xNi_{1-x}O$ a crossover concentration, $x_c = 0.432$, between a ferrimagnetic type ($x < x_c$) and a superparamagnetic regime ($x > x_c$) has been recently reported[23] from a percolation model with Ni clusters, using an Ising model to simulate their magnetic properties, and comparing numerical results obtained by a Monte Carlo technique to experimental data of magnetization measurements and experimental ac susceptibilities. In the $Li_{0.27}Ni_{0.73}O$ crystals ($x < x_c$) studied in this paper, a clear ordered moment is observed (see the hysteresis loops at $T < 40$ K in Figure 6), although an irreversible behavior is observed too.

The results from $Li_{0.27}Ni_{0.73}O$ crystals, like those obtained[11] from a polycrystalline sample with $x = 0.025$, are characteristic of superparamagnetic systems or highly disordered paramagnetic materials. Moreover, a weak ferromagnetic signal starting at 160 K is clearly observed. The dc susceptibility at low field (10 Oe) indicates a very broad maximum at temperatures different from those observed at strong field (1 kOe). Also the ac susceptibility (Figure 7) clearly shows very broad magnetic response in the range 10−60 K, with distinct signatures of absorption in the imaginary part of the susceptibility. These broad components are closer to a superparamagnetic response than to a spin-glass system. The temperature of the weak ferromagnetic component is clearly identified in the ac susceptibility around 160 K by the different frequency response of the real part of the susceptibility. On the other hand, the magnetic behavior of $Li_{0.27}Ni_{0.73}O$ agrees more reliably with the mixed layer structure here determined, than with that including Ni clusters or that based on the alternation of layers fully occupied by either Li or Ni.

Conclusion. After describing how to grow $Li_{0.27}Ni_{0.73}O$ single crystals, in this paper we have reported the crystal structure solution of this material, which has led to the first example of a novel structure type. The more prominent aspect of this model is the mixed quality of the L1 and L2 layers which alternate along the *c* direction containing both Li and Ni in different proportions. This shows that the way in which the Li atom tends to ordinate itself forces the appearance of a new cell and is incompatible with the existence of pure Ni layers alternating with more or less doped Li ones, as it was assumed until now. Evidence on the behavior of $Li_{0.27}Ni_{0.73}O$ as mictomagnetic material has also been presented. The novel structure model here reported looks consistent with the magnetic properties of this material and can throw some light upon the Li diffusion pathway in Li batteries.

Acknowledgment. We acknowledge the financial support of the Spanish DGESIC, Projects MAT99-0892 and PB97-0246, the Fundación *Domingo Martínez*, and the CSIC to the Unidad Asociada GBTYS of the University of Santiago de Compostela.

CM0010203